Highlights (for review)

Click here to download Highlights (for review): crane_bridge_highlights.docx

The paper presents an experimental and numerical investigation of the earthquake response of crane bridges. The main contributions of the authors to this field consist in:

- carrying out an experimental campaign on a model of a crane bridge;
- determining a relevant similarity for the seismic tests which preserves the ratios of seismic forces to friction forces and of seismic forces to gravity forces, without added masses;
- interpreting the experimental results by means of numerical analysis for both low and high excitation intensities;
- proposing a simplified model of the crane bridge which could be used as a part of a bigger model to account for possible interaction between the supporting main structure and the crane bridge.

Experimental and numerical investigation of the earthquake response of crane bridges

Cyril Feau[a], Ioannis Politopoulos[a], George S. Kamaris[a], Charlie Mathey[a], Thierry Chaudat[a], Georges Nahas[b]

[a] CEA, DEN, DM2S, SEMT, EMSI, F-91191 Gif-sur-Yvette, France

[b] IRSN/PSN-EXP/SES/BEGC, 92265 Fontenay aux Roses, France

*corresponding author: tel. :+33169083665, fax : +33169088331, email :ipolitopoulos@cea.fr

Abstract

The experimental and numerical response of crane bridges is studied in this work. To this end, an experimental campaign on a scale model of an overhead crane bridge was carried out on the shaking table of CEA/Saclay in France. A special similarity law has been used which preserves the ratios of seismic forces to friction forces and of seismic forces to gravity forces, without added masses. A numerical model, composed of beam elements, which takes into account non-linear effects, especially impact and friction, and simulates the earthquake response of the crane bridge, is presented. The comparison of experimental and analytical results gives an overall satisfactory agreement. Finally, a simplified model of the crane bridge, with only a few degrees of freedom is proposed.

Keywords: overhead crane bridges, friction, non-linear analysis, seismic tests.

Experimental and numerical investigation of the earthquake response of crane bridges

Cyril Feau[a], Ioannis Politopoulos[a*], George S. Kamaris[a], Charlie Mathey[a], Thierry Chaudat[a], Georges Nahas[b]

[a] CEA, DEN, DM2S, SEMT, EMSI, F-91191 Gif-sur-Yvette, France

[b] IRSN/PSN-EXP/SES/BEGC, 92265 Fontenay aux Roses, France

*corresponding author: tel. :+33169083665, fax : +33169088331, email :ipolitopoulos@cea.fr

Abstract

The experimental and numerical response of crane bridges is studied in this work. To this end, an experimental campaign on a scale model of an overhead crane bridge was carried out on the shaking table of CEA/Saclay in France. A special similarity law has been used which preserves the ratios of seismic forces to friction forces and of seismic forces to gravity forces, without added masses. A numerical model composed of beam elements, which takes into account non-linear effects, especially impact and friction, and simulates the earthquake response of the crane bridge, is presented. The comparison of experimental and analytical results gives an overall satisfactory agreement. Finally, a simplified model of the crane bridge, with only a few degrees of freedom is proposed.

Keywords: overhead crane bridges, friction, non-linear analysis, seismic tests.

1. Introduction

The earthquake response of crane bridges is a very important issue related to safety requirements for industrial facilities and, especially, nuclear plants. Actually, a failure of a component of the crane bridge or of its supports (e.g. supporting steel or concrete runway beams) should be avoided. In addition to the consequences on the handling capacity of the

facility after the earthquake, a major problem may occur if a part of or the whole crane bridge falls on sensitive structures or equipment. Surprisingly, to the authors' knowledge, a very few experimental and analytical research work in this field has been done in the past. The dynamics of elastic continua with moving loads has been covered by Fryba [1] and more recent work presents the approximate analytical solutions [2-6] and finite element solutions [7,8] to similar problems. Regarding the earthquake response of these structures, not many publications can be found in the literature. Komori et al [9] carried out seismic tests under horizontal excitation whereas Otani et al. [10] focused on the vertical earthquake response of a 1/8 scale model. Schukin et Vayandrakh [11] studied the earthquake behavior of a polar crane bridge by means of a comprehensive finite element model. Betbeder et al. [12] and Betbeder and Labbé [13] dealed with simplified models accounting for the reduction of the crane bridge forces due to sliding. Sarh et al. [14] analyzed the behavior of a simplified scale model of a crane bridge subjected to random unidirectional excitation and compared it with experimental tests. More recently, Kenichi et al [15] carried out a shake experimental campaign on a model of a crane bridge focusing on the uplift response of the trolley.

To have a further insight into the earthquake response of crane bridges an experimental campaign of a 1/5 scale model was carried out on one of the shake tables of the Commissariat à l'Énergie Atomique et aux Énergies Alternatives (CEA) in Saclay, France. In the following we describe the most important features of the model, the experimental set-up and we present the main experimental results. Moreover, we discuss some subtle points related to the numerical modeling of the mock-up and we compare the analytical and experimental results.

2. Experimental tests

The mock-up is a simplified 1/5 scale model of a 22.5 m long overhead crane bridge. Given that the shake table is a 6 m x 6 m table, this scale is the biggest scale that could have been considered. The total mass of the unloaded prototype is of about 100 t. The bridge steel girders that support the crane trolley have a rectangular hollow section 1050 mm x 2100 mm. The width of the section flanges and vertical walls are 21 mm and 12 mm respectively. The runway beams are continuous I type steel beams with a typical span of 10 m. The height of the section is 1500 mm, the flanges width and thickness are 600 mm and 35 mm respectively and the web thickness is 12 mm. One important issue for the design of the model was the determination of the similarity law which is presented in the following subsection.

2.1 Similarity law

Due to the limitations in the capacities of the experimental facilities, experimental models are, usually, reduced scale models. To be representative of the behavior of the response of the real structure (prototype), tests on reduced scale models should be carried out following similarity laws. A natural way to do this is through dimensional analysis [16, 17, 18, 19]. Let us look at a quantity of interest, for instance, the vector of relative displacement with respect to the shake table displacement at any point of the bridge, at coordinate $\underline{x}$, $\underline{d}(\underline{x})$. Assuming a homogeneous, isotropic, rate independent material and a Coulomb dry friction for the sliding interfaces, this quantity may be written as a function of the system's parameters:

$$\underline{d} = \phi_d\left(E, \nu, \mu, \underline{x}, t, \rho, g, \underline{\Gamma}, L, ..., \sigma_y, ...L_i...\right) \quad (1)$$

where E is the Young modulus, ν is the coefficient of Poisson, μ is the friction coefficient, t denotes time, ρ is the mass density, $\underline{\Gamma}$ is the vector of shake table acceleration, L is a characteristic length of the structure (e.g. length of the bridge girders). For the sake of

conciseness we limit ourselves only to the above ten variables ($\underline{d}, E, \nu, \mu, \underline{x}, t, \rho, g, \underline{\Gamma}, L$). However, one must keep in mind that several other variables (e.g. nonlinear material properties, other geometrical dimensions like the girders' section dimensions, wheel dimensions etc.), play a role in the system's response. All these are schematically denoted, in the "dot" part into the brackets in equation (1) as, for instance, the yield stress σ_y and other geometrical dimensions L_i. In the present case, the rank of the matrix of the dimensions' exponents of the variables governing the system's response is equal to 3 (i.e. equal to the number of fundamental dimensions: mass, time and length). According to the Vachy-Buckingham's Pi theorem, equation (1) can be written in dimensionless form with *N*-3 dimensionless variables, *N* being the number of the initial variables.

$$\frac{\underline{\underline{d}}}{L} = \Phi_d\left(\nu, \frac{\rho L \underline{\Gamma}}{E}, \frac{E}{\rho L g}, t\frac{\sqrt{E/\rho}}{L}, \frac{\underline{\Gamma}}{\mu g}, \frac{\underline{x}}{L}..., \frac{\sigma_y}{E}, ...\frac{L_i}{L}...\right) \qquad (2)$$

A similar relation holds if the quantity of interest is the dimensionless stress $\underline{\underline{\sigma}}/E$ instead of the dimensionless displacement. The products $\Pi_1 = \rho L \underline{\Gamma}/E$ and $\Pi_2 = E/\rho L g$ may be seen as the ratios of seismic excitation forces to elastic forces and of elastic forces to gravity forces respectively. The latter is the Froude number. The dimensionless time $\Pi_3 = t\sqrt{E/\rho}/L$ is the ratio of time to the time needed by sound waves to travel over the length *L*. $\Pi_4 = \underline{\Gamma}/(\mu g)$ accounts for the ratio of the seismic excitation forces to the friction forces.

A complete similitude is achieved if all dimensionless variables have the same values for both the model and the prototype. In the framework of seismic tests of structures two similarity laws are widely used: velocity similarity and, even more frequently, Froude or gravity similarity. Consider a uniform geometrical scaling, that is, the coordinates of the

model and of the prototype (scale 1 structure) satisfy the relation $\underline{x} = \lambda \underline{x}_0$, where λ denotes the scaling factor (1/5 in this case) and subscript 0 denotes, throughout this paper, quantities referred to the prototype. According to the velocity similarity law, all dimensionless products in equation (2) are the same for the model and the prototype, except the Froude number Π_2. If the same material (E, ν, ρ) is used for both the prototype and the model, the above similarity implies that the time scaling is $t/t_0 = \lambda$ and the ratios of mass, M, stiffness, K and eigenfrequencies, f, of the model to those of the prototype are:

$$M/M_0 = \lambda^3, K/K_0 = \lambda, f/f_0 = 1/\lambda \quad (3)$$

Π_3 and Π_1 similitude imply that the time scaling is $t/t_0 = \lambda$ and that the excitation (table) acceleration components, Γ, must be amplified by the reciprocal of the scaling factor i.e. $\Gamma(t)/\Gamma_0(t_0) = 1/\lambda$. The resulting displacement, velocity and acceleration components, respectively d , v and a, vary as:

$$d(t)/d_0(t_0) = \lambda, v(t)/v_0(t_0) = 1, a(t)/a_0(t_0) = 1/\lambda \quad (4)$$

This law is called velocity similarity because there is no velocity scaling. It is well known that the main drawback of this similarity law is that, since the Froude number similitude is not satisfied, the ratio between dynamic and static stresses of the model is not the same as in the prototype.. Moreover, in the present case, where the importance of friction phenomena is crucial, if the same coefficient of friction μ, is used for both the prototype and the model, it is not possible to respect Π_4 similarity. Therefore, similarity of the friction forces with respect to the seismic excitation forces cannot be achieved unless specific interface materials are used with a friction coefficient $1/\lambda$ times the friction coefficient of the prototype. Given that steel

to steel friction coefficient is of about 0.20 this would imply a model friction coefficient of about 1 which is hardly feasible if not impossible.

The most frequently used similarity law, in experimental earthquake engineering, is the gravity or Froude similarity. In this case, all the dimensionless variables in equation (2), including the Froude number, are the same for the model and the prototype. This results in the following similarity relations:

$$\rho/\rho_0 = 1/\lambda \ \ , K/K_0 = \lambda, f/f_0 = 1/\sqrt{\lambda},$$

$$t/t_0 = \sqrt{\lambda}, \Gamma/\Gamma_0 = 1,\ d/d_0 = \lambda,\ v/v_0 = 1/\sqrt{\lambda},\ a/a_0 = 1 \qquad (5)$$

This similitude law respects similarity of the ratios of friction and gravity forces to seismic excitation forces. However, the necessary condition to meet this requirement is that the mass density ρ, should be changed leading to $M/M_0 = \lambda^2$ instead of $M/M_0 = \lambda^3$. In many cases, for instance buildings' models, this is achieved, in practice, by adding additional masses on the slabs of the mock-up. However, adding masses, all over the crane bridge beams, would be not only practically complicated, but it would, also, have a considerable impact on the stiffness of the crane bridge. Actually, since $\lambda = 1/5$, the added masses should be four times the mass of the bridge itself. It is obvious that such rigid heavy blocks, put one next to the other to increase the mass of the beams, would have, inevitably, increased also the beams' stiffness, since they should be tightly attached to the beams to avoid sliding.

To by-pass this problem, we have decided to follow another similarity law, specifically determined for these tests. The goal is to obtain, as much as possible, the same similarity relations given by the gravity similarity without adding masses or changing the material properties of the bridge beams. To this end, the hollow section of the model bridge beams is not just a geometrically scaled section of that of the prototype. In fact, it can be considered that the deformability of the bridge girders is governed, mainly, by their bending

flexibility. That is, the governing parameters are their section moments of inertia. Of course this is true so far as the beam material remains elastic. As it was confirmed, a posteriori, by the analytical and experimental results, yielding does not occur for the considered excitation intensities. Hence, equation (1) may be modified as follows:

$$\underline{d} = \tilde{\phi}_d\left(E, \nu, \mu, \underline{x}, t, \rho, g, \underline{\Gamma}, L, S, I_y, I_z, ...\right) \qquad (6)$$

where S denotes the section area and I_y and I_z denote the section moment of inertia with respect to axis y and z respectively. Applying the Pi theorem, the dimensionless equation reads:

$$\frac{\underline{d}}{L} = \tilde{\Phi}_d\left(\nu, \frac{\rho SL^3\underline{\Gamma}}{EI_y}, \frac{\rho SL^3\underline{\Gamma}}{EI_z}, \frac{\rho L^3\underline{\Gamma}}{ES}, \frac{EI_y}{\rho SL^3 g}, \frac{EI_z}{\rho SL^3 g}, t\sqrt{\frac{g}{L}}, \frac{\underline{\Gamma}}{\mu g}, \frac{\underline{x}}{L}, ...\right) \qquad (7)$$

If the quantities of interest are the bending moments or reaction forces $\underline{M}$ and $\underline{R}$ respectively , a similar relation holds for their dimensionless counterparts $\underline{M}/(\rho SL^2 g)$ and $\underline{R}/(\rho SLg)$.. Since equation (6) has three more variables than equation (1), there are nine dimensionless variables in equation (7) instead of six in equation (2). It is worth noting that the ratio of elastic forces to seismic forces used in equation (2), Π_1, is, now, replaced by three ratios, $\tilde{\Pi}_1 = \rho SL^3\underline{\Gamma}/(EI_y)$, $\tilde{\Pi}_2 = \rho SL^3\underline{\Gamma}/(EI_z)$ and $\tilde{\Pi}_3 = \rho L^3\underline{\Gamma}/(ES)$. The same holds, also, for the ratio of elastic forces to gravity forces which is represented by two dimensionless products $\tilde{\Pi}_4 = EI_y/(\rho SL^3 g)$ and $\tilde{\Pi}_5 = EI_z/(\rho SL^3 g)$ instead of one, Π_2, in equation (2). The dimensionless time is also defined in a different way, as $\tilde{\Pi}_6 = t\sqrt{g/L}$. As already mentioned, we consider that the deformation of the bridge is governed by bending and phenomena

associated to longitudinal dynamics are less important. Therefore, we do not apply $\tilde{\Pi}_3$ similitude. To meet the requirements imposed by the products $\tilde{\Pi}_1$, $\tilde{\Pi}_2$, $\tilde{\Pi}_4$ and $\tilde{\Pi}_5$, we seek a hollow section with height h, width b, and thickness e, so that $S/S_0 = \lambda$ (instead of $S/S_0 = \lambda^2$), $I_y/I_{y0} = \lambda^4$ and $I_z/I_{z0} = \lambda^4$. The resulting non-linear system was solved with a Newton-Raphson method and gave $h = 250$ mm, $b = 110$ mm and $e = 30$ mm.

As in the case of Froude similitude, respect of the dimensionless time $\tilde{\Pi}_6$, implies $t/t_0 = \sqrt{\lambda}$ which is consistent with the bending frequencies similarity, $f/f_0 = 1/\sqrt{\lambda}$. This time contraction is smaller than that implied if Π_3 is considered (i.e. $t/t_0 = \lambda$). Regarding the two runway beams, we focused on similarity related mainly to their horizontal bending stiffness, which gives IPN 240 type beams.

The above similarity is equivalent to the gravity similarity as far as bending behavior is concerned only. In fact, special care has been taken only for bending stiffness but the axial stiffness does not vary proportionally to λ. However, distortion of the axial stiffness is not a concern for the structure of interest since motions with considerable axial deformations are quite high frequency motions, beyond the excitation frequency content. It is, also, worth noting that though the correct similarity relation is obtained for bending moments ($\propto \lambda^3$) and reaction forces ($\propto \lambda^2$), stresses in the model are lower than those in the prototype. This is due to the fact that, since $S/S_0 = \lambda$, the sections of the model are bigger than those that would have been obtained by uniform geometrical scaling ($S/S_0 = \lambda^2$).

2.2 Experimental set-up

As already mentioned the mock-up is a simplified 1/5 scale model of the prototype, made of steel with yield stress equal to 355 MPa. The sections of the bridge girders (beams supporting the trolley) and of the runway beams, supporting the whole bridge, are described

in the previous subsection. Their lengths are 5 m and 2 m respectively. The distance between the central axes of the bridge girders is 50 cm. The beams linking the two main bridge girders (end trucks) have a box type section 110 mm x 320 mm and their length is equal to 0.8 m. The thickness of the section flanges and vertical walls is 30 mm. The trolley is a rigid mass of 1880 kg. The total mass of the mock-up, including the runway beams, is about 3.9 t. The trolley and the bridge are supported by four wheels each. The wheels can be blocked or let free to roll. Actually, in real crane bridges, the drive wheels (those connected to the motor) are blocked when the motor is turned off. Several sensors, mainly, accelerometers and displacement transducers were mounted on the mock-up. In figure 1 a view of the model mounted on the shake table is depicted together with the axes of the reference frame considered in the experimental campaign and the work herein. A detailed description of the model and of the whole experimental set-up can be found in [20].

2.3 Experimental Campaign

A comprehensive experimental campaign has been performed using the above described model. Special care was taken to identify step by step the model dynamic properties which would be useful to the accurate determination of the characteristics of the analytical model also. To this end, modal analysis tests, with shock hammer, were carried out of the subassembly composed of the main bridge girders only. This structure was put on very low stiffness pneumatic springs, resulting in free end boundary conditions. Twenty three-dimensional accelerometers were mounted on this subassembly to obtain its nine first mode shapes and frequencies. The results of the modal analysis are presented in figure 2.

Then, several configurations of the whole crane bridge, corresponding to different trolley locations and different wheel conditions (braked or free to roll) have been considered. At the beginning, low intensity white noise acceleration signals were applied to the table. The

aim of these low intensity tests was to identify the characteristic properties of the model when the response is, as much as possible, close to linear response. Assuming linear behavior (i.e. sticking contact conditions for the braked wheels), these low intensity tests were used to determine the initial eigenmodes of the system.

Eventually, seismic excitation signals were considered. Seismic signals should be compatible with the earthquake motions of the crane bridge supports. Actually, the applied excitations must correspond to the ground excitation filtered by the response of the building housing the crane bridge. Nevertheless, due to the uncertainties related to the computation of floor motions, ground signals were considered. Though this type of excitation may be theoretically controversial, the experimental results are still very relevant since they give useful information on the earthquake response of crane bridges and they can be used to validate numerical simulation codes and methods. The applied signals were artificially generated signals compatible with the response spectrum of the Marcoule nuclear plant site, in south France. The use of artificial signals, matching a given spectrum, is not, in general, recommended for nonlinear problems as the problem in hand. Nevertheless, such signals were considered here for the following reasons: a) lack of available real records compatible with the actual site conditions b) the target spectrum is a spectrum determined after a specific seismological study of the site. Hence it is narrower than commonly used regulations spectra and c) it may reasonably and intuitively, though not mathematically rigorous, be expected that artificial signals would be, in general, more “severe” than real records, whose spectra fit partially or lie under the target spectrum, provided their duration is not too small. In fact, because of their unrealistic, wider frequency content, artificial signals will have more energy over the whole frequency range of interest than real records and thus they will be more demanding for structures exhibiting frequency shift due to nonlinear response.

The generated signals were scaled to peak ground accelerations (PGA) equal to 0.2g, 0.4g and 0.8g. For similitude reasons a time contraction of $\sqrt{5}$ was applied to all the excitation signals. Tests under mono-axial, bi-axial (horizontal) and tri-axial (horizontal + vertical) excitations were carried out. In the following, input acceleration signals in x, y and z direction are noted Γ_x, Γ_y and Γ_z respectively. Figure 3 shows the time histories of Γ_x and Γ_y for the case of a PGA equal to 0.8g. For lack of space, only the results of few tests will be presented herein. The results of all tests can be found in [20].

3. Numerical model

In most analyses, done by practitioners, beam type elements are used for the numerical modeling of crane bridges. Actually, nonlinear dynamic analyses with beam element models can be run in much shorter time than more complex shell or brick elements models. Therefore, our goal was to determine a numerical model composed of beam elements which would represent accurately the earthquake response of the crane bridge. Analyses were carried out with the homemade finite element (FE) code CAST3M [21].

3.1 Runway beams

The runway beams are IPN 240 beams having a span of 2 m. They are fixed on the table plate by means of stiffened plates which are deemed to account for clamped end conditions (figure 4). At a first glance, one could think that the important issue is the lateral bending flexibility of the runway beams which can be accurately taken into account by classical beam elements. However, torsion is induced by the horizontal transverse wheel forces which are applied on the rail, at the top of the beam. Torsion stiffness for this kind of sections is due, mainly, to warping stiffness (i.e. lateral bending of the upper and lower flanges). On the other hand classical beam elements account only for St. Venant torsional stiffness which is much

lower than the warping stiffness in the present case. Moreover, computations revealed that, contrary to intuition, the boundary plates did not impose purely clamped conditions. Therefore a brick finite element model was used to determine accurately the flexibility of the runway beams subject to the wheel forces.

To highlight the influence of the flexibility of the boundary plates the lateral (in the x direction) stiffness K of a runway beam subjected to two horizontal forces at the wheels' locations was determined by two different static computations. The results presented here correspond to configurations where the initial wheels' position is symmetrical with respect to the mid-span of the runway beams. For the first analysis, the supports of the beams were modeled in detail to represent the actual boundary conditions. For the second analysis, the runway beam was supposed to be perfectly clamped at the two ends of its span. The deformed shapes of the runway beam, resulting from the two static analyses are shown in figure 4. An estimate of the frequency f_x of the first mode of the bridge in the x direction is:

$$f_x = \frac{1}{2\pi}\sqrt{\frac{2K}{M}} \qquad (8)$$

where M is the total mass of the bridge. Taking into account the boundary flexibility resulted in a frequency of 9.5 Hz, whereas perfectly clamped conditions lead to a frequency of 11.5 Hz. The first result is in accordance with the frequency value obtained experimentally. It is also observed in figure 4 that the flanges of the runway beam deform so that the usual assumption of beam theory that sections do not exhibit in plane deformation is no longer valid.

For the above reasons, it is obvious that runway beams cannot be modeled with classical beam models. To reduce the size of the final problem, assembling all bridge components, a Guyan reduction (static condensation) has been done so that each runway

beam model was reduced to a 12×12 matrix at the two contact points of the wheels with the rail. Such a reduction assumes that the location of the contact points between the wheels and the rail will not change significantly during the earthquake response of the bridge. This assumption is consistent with the small sliding displacements observed experimentally. It has, also, been verified a posteriori by the analytical results.

3.2 Bridge beams connections

At the beginning the bridge was modeled as an assembly of four beams: the two girders supporting the trolley and the two short transverse beams supporting the wheels (end trucks). As already mentioned in subsection 2.3, to validate the numerical model a modal identification of this assembly was carried out. Comparison between the experimental and the analytically computed eigenfrequencies showed that the numerical model based on beam elements was much stiffer than the mock-up.

To understand the higher flexibility of the actual model, a shell element model of the end truck has been done and a rigid body rotation of the nodes at the interface with the beam girder was imposed. In the case of symmetrical imposed rotations (i.e. zero rotation at the mid-span of the end truck) a rotational stiffness of $1.08\ 10^7$ Nm/rad was found. If E, I, L are the Young modulus, the moment of inertia and the length (distance between the axes of the bridge girders) of the end truck beams respectively, the stiffness according to the beam theory is $2\,EI/L = 2.31\ 10^7$ Nm/rad. The increased flexibility (reduced stiffness) of the mock-up joint and of the shell element model may be understood with a look at figure 5. In fact, it is observed that, the longitudinal axial stress distribution in the internal wall of the end truck is consistent with beam theory (constant all over the height of the section wall) only after a certain distance from the interface with the girder. This observation is in agreement with St. Venant's principle and shows that, in the vicinity of the imposed rotation, only a part of the

internal section wall contributes to the bending stiffness. This joint flexibility cannot be taken into account by the beam element model. Therefore, on the basis of the above analysis, rotational springs, in the horizontal plane, have been considered at the joints of the bridge beams. Their stiffness has been determined either from the shell finite element model or by trial and error seeking that the first computed eigenfrequency of the beam element model is equal to the first experimental eigenfrequency. It turned out that both methods gave the same rotational stiffness value, $1.08\ 10^7$ Nm/rad. For the same reasons, torsional springs have also been inserted between the beam girders and the end trucks to account for the increased torsional flexibility of the girders compared to that of a classical beam element model. A very good agreement with the eigenshapes and eigenfrequencies obtained by hammer tests is observed for the first nine eigenmodes, up to 110 Hz. This illustrated, for the first two eigenmodes in figure 2.

The trolley, moving on the crane bridge girders, is modeled as a rigid body having overall dimensions and mass equal to those of the actual trolley utilized of the mock-up.

3.3 Contact nonlinearities

The finite element model accounts for non-linear effects, especially impact and friction, which are the most important nonlinearities of the problem of interest. In the finite element model each wheel is represented merely as a node of the model. There is no special finite element mesh or other specific model of the wheels. Impact and friction are modeled by penalty methods similar to those in [22, 23]. Normal impact force is proportional to the penetration of the impacting node multiplied by an interface contact stiffness. A damping term is also added to account for a restitution coefficient less than one. Regarding friction, the classical elastoplactic penalty method is used [22]. The tangential force varies with respect to the sliding relative displacement according to an elastic perfectly plastic law. The yielding

force (i.e. sliding force) is equal to the instantaneous normal force multiplied by the friction coefficient. To simulate possible sticking during impact, the characteristic time associated to the tangential motion must be sufficiently shorter than the characteristic time associated to the normal motion. This means that the tangential penalty stiffness must be sufficiently higher (about 10 times) than the normal penalty stiffness. Moreover, to simulate no penetration conditions, penalty stiffness should be, in general, much higher than the other terms of the structural stiffness matrix. On the other hand, too high penalty stiffness may cause convergence difficulties of implicit algorithms or imply a very small time step in the case of explicit algorithms. To determine the optimum values of the penalty stiffness, we compared two linear models. One, assuming fixed connection, between the wheels of the trolley and the bridge and the supporting bridge girders and runway beams respectively. Another model is also built, but, this time, the above connections were modeled by means of penalty springs. The minimum values of the penalties' stiffness giving the same eigenmodes up to a frequency of 200 Hz were retained as the optimum penalties stiffness. Actually, compliance with the above criterion demonstrates that the considered penalties' stiffness is high enough to account for sticking conditions in the range of frequencies of practical interest.

Regarding friction, another alternative, which has been used in this work, is the nonlinear damping penalty method proposed in [23]. The Coulomb dry friction law is regularized as follows:

$$\boldsymbol{F}_T = -\mu N \left[2 - \frac{|\dot{\boldsymbol{u}}_r|}{\epsilon}\right] \frac{\dot{\boldsymbol{u}}_r}{\epsilon} \qquad \text{if } |\dot{\boldsymbol{u}}_r| < \epsilon \tag{9}$$

$$\boldsymbol{F}_T = -\mu N \frac{\dot{\boldsymbol{u}}_r}{|\dot{\boldsymbol{u}}_r|} \qquad \text{if } |\dot{\boldsymbol{u}}_r| \geq \epsilon \tag{10}$$

where N is the normal force, μ is the friction coefficient $\dot{\boldsymbol{u}}_r$ is the relative tangential velocity. The adherence friction force is approximated by a nonlinear damping type force for sliding velocities lower than a small tangential velocity threshold, ϵ. The value of ϵ is a tradeoff between accuracy and computational time. This parameter should be chosen so that a sliding velocity equal to ϵ can be considered as a very low velocity for the problem of interest, corresponding, practically, to a sticking phase. On the other hand, similarly to penalty stiffness, too small values of ϵ (high penalty damping) would increase the computational effort.

The above models are adequate for the modeling of braked wheels. However, the situation is different for rolling wheels. In fact, when a wheel is rolling, the friction force in the rolling direction is very low and can be neglected. However, this is not the case in the perpendicular direction. One could think that the remedy would be an anisotropic friction model with two different sliding coefficients in x and y directions. It turns out that such models cannot give the right solution because they are not consistent with the physics. Actually the contact point of a rolling wheel is in adherence (i.e. sticking) phase and its behavior cannot be simulated considering sliding conditions. To address this issue a macro-element taking into account the kinematics of a wheel and the correct sticking and sliding conditions should be used. The development of such a macro-element will be done in future work.

4. Experimental results and interpretation

In this section we focus on the capacity of the above numerical model to interpret the experimental results. In a first step it is checked if the finite element model is capable to reproduce the experimental results under low intensity excitation i.e. in the case of quasi-linear behavior of the bridge. Then, the numerical simulation of the test at the highest

excitation level was carried out and compared to the measured response. In addition the sensitivity of the results either to input uncertainties (e.g. value of the actual gap between the wheels and the rails) or to modeling assumptions (e.g. beam finite model which does not take into account the additional flexibilities discussed in subsections 3.1 and 3.2) has been investigated.

In all cases considered here, the initial configuration of the crane bridge was that presented in figure 6. The trolley and the end trucks were located at the mid span of the bridge girders and the runway beams respectively. The braked wheels of the trolley and the bridge were symmetrical with respect to their respective axes of motion.

4.1 Model validation for quasi-linear behavior

In the case of quasi-linear behavior, a two-step validation of the numerical has been done. First, the eigenfrequencies and eigenshapes computed by a linear model (i.e. without impact/friction nonlinearities, assuming sticking conditions) of the bridge were compared to those obtained experimentally under low intensity white noise excitation. Regarding the experimental modal identification, the underlying assumption was that the excitation amplitude was sufficiently low, so that non-linearities could be neglected. The agreement between the eigenmodes obtained numerically and experimentally was very satisfactory.
Then, the above results were compared to those given by a nonlinear analysis of the bridge subjected to the shake table white noise excitation. A satisfactory agreement was obtained, demonstrating the capacity of the nonlinear model to capture the essential features of the response at the limit, when the response is quasi-linear.

The first three eigenmodes and frequencies of the crane bridge model are shown in figure 7. The indicated predominant direction is that corresponding to the higher effective mass. The analytically and experimentally determined eigenfrequencies are almost identical

except the first vertical eigenfrequency which is slightly overestimated by the numerical model. The effective masses of these modes in the *y*, *x* and *z* directions are equal to 73%, 98 % and 86% of the total mass respectively.

4.2 Nonlinear behaviour

To investigate the capacity of the analytical model to predict the nonlinear earthquake response of the crane bridge experimental and analytical results were compared in the case of a high excitation intensity. During this test the model was subjected to a bi-axial shake table excitation with a peak ground acceleration (PGA) of 0.8g.

As for the numerical simulations, the Oden's and Martins' [23] model was used with a value of the regularization velocity, ϵ, equal to 10^{-3} m/s and the impact penalty stiffness values were determined according to the procedure described in the subsection 3.3. The computations were performed with a friction coefficient equal to 0.23 for the braked wheels, which is a typical friction coefficient value for steel to steel interfaces. Moreover this friction coefficient is consistent with the observed experimental results. Actually, the measured acceleration of the trolley in direction *x* is saturated at about 0.12 g which correspond to an apparent friction coefficient of 0.12. Since only two of the four wheels are braked, the actual friction coefficient is about twice the apparent friction coefficient. A very low (0.02) friction coefficient has been considered for the rolling wheels. A critical damping ratio of 3 % was considered for all eigenmodes of the crane bridge substructures with free boundary conditions at their points of contact with the other components (e.g. contact points between the wheels of the bridge and the runway beam or between the girders and the wheels of the trolley). The measured value of the initial gap between the wheels and the rails was 2 mm.

Particular attention must be drawn to the well-known sensitivity of sliding displacement to the low frequency content of the excitation signal. In figure 8 the mean

horizontal displacement in y direction of the end trucks is shown for three pairs of horizontal excitation signals. These excitation signals are identical except a $\pm$ 0.01 g shift of their time average values, $\langle\Gamma_x\rangle$ and $\langle\Gamma_y\rangle$. This shift is consistent with the measurement noise of the accelerometers. It may be observed that even such a slight offset leads to considerable discrepancies of the responses. The consequence of the inherent uncertainties, even small, of the measurements of the low frequency excitation components is that sliding displacements cannot be predicted accurately. It is, also, worth noting that in the case of a zero mean excitation signal, the bridge slides more in direction $+y$. This is due to the asymmetry of the contact conditions (figure 6). In fact, because of the moment due to the vertical eccentricity of the mass, the vertical forces on the braked and on the free to roll wheels are not the same. When the vertical forces on the free to roll wheels are higher than those on the braked wheels, the friction force opposed to the motion is lower than in the contrary case. This kind of asymmetric sliding response towards the side of the free to roll wheels was also observed in real crane bridges. Though not shown here, a similar asymmetric sliding behavior of the trolley in direction $-x$ is also observed. Figure 8 demonstrates, also, that, depending on its sign, the offset of the excitation signal increases further or decreases the above asymmetric sliding under zero mean excitation.

Because of the above sensitivity, sliding displacement is not a relevant quantity for the comparison between analytical and experimental results. Therefore, the comparison focuses on absolute accelerations and on the overall girder's deformation. Furthermore, comparison of the acceleration time histories would not have been very meaningful, due to the well-known sensitivity of sliding systems' response. In our opinion, comparison in the frequency domain is better suited for drawing, at least, qualitatively conclusions.

Figure 9 to figure 11, show the pseudovelocity response spectra computed from the absolute experimental and analytical accelerations of the bridge for a critical damping ratio of

1%. This kind of spectra have been preferred to Fourier spectra of the accelerations to avoid the highly oscillatory behavior of Fourier spectra. For the sake of completeness, the pseudovelocity response spectra of the shake table acceleration are also shown in these figures. It may be observed that the analytical model captures, qualitatively, the essential features of the experimental results for the different bridge components. Figure 9 shows that the analytical model results in a lower pseudovelocity response spectrum of the runway beams in direction x. Because of the high rigidity of the runway beams in direction y, the agreement between analytical and experimental results in that direction is much better. In fact, it is observed that all three spectra are quasi-identical, except in the low frequency range. Regarding the response of the girders (figure 10), the analytical model gives satisfactory results in both horizontal directions. As for the trolley, figure 11 shows a very good agreement between experimental and analytical results in direction x, whereas the agreement in direction y is less satisfactory, especially in the frequency range between 7 Hz and 16 Hz. Though not shown here, for the sake of conciseness, the analytical model gives good results for the absolute accelerations measured on the end trucks also. As a general trend, the pseudovelocity response spectra values of the different bridge components, except the trolley, are of the same order of magnitude as the pseudovelocity response spectrum of the excitation..

The bending moment and stresses in the bridge girders due to horizontal bending are important quantities for the assessment of the earthquake behavior of crane bridges butthey were not directly measured during the test. Therefore, the capability of the numerical model to estimate accurately the girders' stresses was confirmed comparing the analytical and experimental relative horizontal displacements of the girder's mid span with respect to the end truck displacements. Actually, this quantity characterizes the overall horizontal bending deformation of the girders. It is worth noting that the two end trucks do not exhibit the same displacements. Consequently their mean displacement must be determined. Even though the

time histories of the analytical and experimental displacements are not identical, the agreement may be considered as satisfactory, especially as far as the maximum relative displacement is concerned. In fact, the maximum relative displacement amplitudes given by the analytical model and measured experimentally are, both, about 1.3 mm. Therefore, given the capability of the analytical model to predict the correct deflection amplitude, the axial stresses can be estimated analytically. It is found that the maximum axial stress, due to both dynamic and static loadings, is equal to 21.4 MPa. Since the yield stress of the utilized steel is 355 MPa no yielding occurs and the assumption of material linearity is verified.

4.3 Model sensitivity

To have a better understanding of the influence of input uncertainties or of the numerical modeling approximations, two supplemental analyses were done. First, an analysis was carried out considering a zero gap between the wheels and the rails. In fact, the actual gap value may not be known with accuracy. Even more, it could be thought, that, at high excitation level, the exact gap value is of no importance. Thus, the limit case for which the gaps are zero has been studied. Another analysis was also done using a beam finite element model which does not account for the increased local flexibilities discussed in subsections 3.1 and 3.2. In this model each runway beam was modeled as a classical beam clamped at both ends. However, its torsional constant has been adjusted so as to account for the warping torsion effect. Without this adjustment, the first eigenfrequency in direction x would have been 14 Hz instead of the actual value of 9.5 Hz (figure 4). No additional rotational springs were inserted at the connections between the bridge girders and the end trucks. Actually, it is likely that the finite element models, made by practitioners, will not be tuned as the reference model, described in subsections 3.1 and 3.2. Regarding modal analysis of the above no-tuned model, the first three frequencies of the eigenmodes in y, x and z directions are 11.0 Hz, 11.7

Hz and 14.5 Hz respectively. Comparison with the values determined either experimentally or with the reference analytical model (figure 7) reveals an overestimation of the frequencies varying from 11% to 23%.

Regarding the nonlinear test at the 0.8g PGA level, the results of the analyses are summarized in table 1. These results show that, regardless of the model (i.e. reference or no-tuned models), the maxima of the horizontal bending moment, of the relative displacement of the girder mid span and the sliding displacement in the y direction, are higher when the gaps are equal to zero. In this case, impact between the trolley wheels and the girder's rail occurs much more often and gives rise to higher impact force than in the case of 2 mm gap. It may, also be observed that the average horizontal bending moment value is not zero, especially in the case of zero gap. In fact, the horizontal dynamic loading of an individual girder does not have zero mean because of the unilateral constraints between the trolley and the girder. An approximate estimate of the average bending moment could be given by the formulae giving the bending moment at the mid span of a clamped-clamped beam under a concentrated force, equal to the average impact force applied at the same point (i.e. $\langle M(t)\rangle = \langle F(t)\rangle L/8$ where $M(t)$ is the bending moment, $F(t)$ is the trolley impact force, $\langle . \rangle$ denotes time average value and L the length of the bridge girder). This approximation is confirmed by the results of table 1. Though, as mentioned in the beginning of this subsection, the grosser, no-tuned model, is not very accurate in the case of quasi-linear behavior, nonlinearities tend to decrease, to some extent, the differences between the two models.

In addition to the above analyses, related to input uncertainties and modeling approximations, another analysis was also carried out using a linear model of the crane bridge, assuming sticking contact conditions for the braked wheels, even in the case of high excitation intensity. The reason is that, even nowadays, the use of linear models for the assessment of the earthquake behavior of crane bridge is common practice. The aim of this

analysis was to highlight the differences between linear and nonlinear responses. For this kind of analysis, a modal critical damping ratio of 0.7 % is considered, instead of 3% for the nonlinear case. The reason for considering this lower damping value is explained in the following section, dealing with the simplified model. As it can be seen in figure 12, accelerations given by the linear model are much higher than those given by the nonlinear model. This may be readily explained by the fact that sliding acts as a sort of seismic isolation. Though not shown here, the same holds for stresses, which are overestimated by the linear model by about 300 %. It is, also, observed that, as expected, nonlinearities result in much wider spectra than linear spectra which exhibit amplification in narrow frequency ranges in the vicinities of the eigenfrequencies of the structure.

Another test at high horizontal excitation level (0.8g PGA) was also done but a vertical excitation (0.53g PGA) was also added. Figure 13 compares the experimentally and analytically obtained response spectra of the trolley's vertical acceleration. It is observed that the peaks on these spectra are slightly shifted towards lower frequencies if compared to the eigenfrequencies presented in figure 7c. The frequency of the peak corresponding to the analytical model is about 10% higher than that corresponding to the test. This slight discrepancy is comparable to that between the eigenfrequencies of the analytical and experimental model. As for the response in the horizontal directions, not shown here, for lack of space, a good agreement is obtained between analytical and experimental results.

5. Simplified model

In this subsection a simplified model of the crane bridge is presented. It aims at giving a quick estimate of the bridge response under bi-axial horizontal excitation. It could also be used as a part of a model including both the support main structure and the crane bridge to account for possible interaction between these two structures. Figure 14 shows the

components of this model which has five intertial DOFs. It is composed of the trolley with mass m_{tr}, the crane girders with mass m_{gi}, stiffness k_{gi}, and damping c_{gi}, and the end trucks having an equivalent mass m_e. In addition springs k_x and damper dashpots c_x represent the stiffness and damping of the runway beams. Mass m_{gi} is not the physical mass of the bridge girders but it is chosen so that $m_{gi} + m_{tr}$ is equal to the effective mass of the first horizontal flexural mode of the crane bridge, considering sticking conditions for the braked wheels of the end trucks and the trolley. The stiffness k_{gi} and damping c_{gi} are chosen so that the corresponding frequency and critical damping ratio are those of the above first horizontal flexural mode of the crane bridge.

Particular attention must be paid to the determination of the damping value. Actually, as mentioned in subsection 4.2, the damping taken into account in the finite element model was a critical damping ratio of 3 % for all eigenmodes of the crane bridge substructures with free boundary conditions. However, in the case of the simplified model, the first eigenmode with sticking conditions is considered, thus the damping value will be different. Let us denote $\boldsymbol{\varphi}_n$ and $\tilde{\boldsymbol{\varphi}}_1$ the *n*th of *N* eigenvectors determined under free boundary conditions and the first eigenvector under sticking conditions respectively. In the coordinate basis $\boldsymbol{\varphi}_n$, $\tilde{\boldsymbol{\varphi}}_1$ reads:

$$\tilde{\boldsymbol{\varphi}}_1 = \sum_{n=1}^{N} \frac{\boldsymbol{\varphi}_n^T \boldsymbol{M} \tilde{\boldsymbol{\varphi}}_1}{m_n} \boldsymbol{\varphi}_n \qquad (11)$$

where $\boldsymbol{M}$ is the mass matrix of the bridge, without the trolley mass and m_n is the generalized mass of the *n*th eigenmode under free boundary conditions. The dissipated power corresponding to a unit generalized velocity of the first mode under sticking conditions (i.e. a velocity field equal to $\tilde{\boldsymbol{\varphi}}_1$) reads:

$$2\tilde{\xi}_1\tilde{\omega}_1\tilde{m}_1 = \tilde{\boldsymbol{\varphi}}_1^T\boldsymbol{C}\tilde{\boldsymbol{\varphi}}_1 = \sum_{n=1}^{N}\left(\frac{\boldsymbol{\varphi}_n^T\boldsymbol{M}\tilde{\boldsymbol{\varphi}}_1}{m_n}\right)^2\boldsymbol{\varphi}_n^T\boldsymbol{C}\boldsymbol{\varphi}_n = 2\sum_{n=1}^{N}\frac{\left(\boldsymbol{\varphi}_n^T\boldsymbol{M}\tilde{\boldsymbol{\varphi}}_1\right)^2}{m_n}\xi_n\omega_n \quad (12)$$

where $\boldsymbol{C}$ is the damping matrix, assumed to be diagonalizable in the basis $\boldsymbol{\varphi}_n$, ξ_n, ω_n and m_n are the critical damping ratio and the circular frequency of the *n*th eigenmode under free boundary conditions and $\tilde{\xi}_1$, $\tilde{\omega}_1$ and $\tilde{m}_1$ are the critical damping ratio, the circular frequency and the generalized mass of the first eigenmode under sticking conditions. For the case in hand, with $\xi_n = 0.03$, which was the damping considered in subsection 4.2 for the eigenmodes with free boundary conditions, the critical damping ratio of the simplified model, given by equation (12), is $\tilde{\xi}_1 = 0.7$ %.

The total mass of the bridge, including the masses of the girders, the trolley and the end trucks is $m_t = 3648$ kg. The equivalent mass of the end trucks is not their physical mass but $m_e = m_t - m_{gi} - m_{tr}$. The trolley (mass m_{tr}) can slide with respect to the bridge girders (mass m_{gi}). The friction coefficient is the mean friction coefficient of the four wheels used in the FE model. Only two over four wheels are braked. Reminding that friction coefficients equal to 0.23 and 0.02 for braked and free to roll wheels, respectively, have been considered (section 4.2) a mean friction coefficient $\mu = (0.23 + 0.02)/2 = 0.125$ is assumed. This friction coefficient accounts for horizontal friction of the horizontal interface between the wheels and the girder's rail. Impact and horizontal friction on a vertical interface occurs, also, when the gap between the wheels and the rail is zero. The corresponding friction coefficient is 0.23.

The bridge base (end trucks with mass m_e) can slide with respect to the points representing the runway beams. Regarding the friction coefficient of the horizontal interface the same average friction coefficient as for the trolley is considered. In addition, unilateral horizontal frictional impact conditions are also imposed between mass m_e and the springs and

dampers modeling the runway beam. The spring stiffness, k_x, is such that the frequency in x direction is equal to that obtained by the FE model. The damping constant, c_x, is determined to match the assumed Newton's restitution coefficient, r. For the examples treated here $r = 0.7$ is assumed. For this vertical interface, the same friction coefficient, $\mu = 0.23$, as in the FE model is used. The values of the main parameters of the model are summarized in table 2.

The underlying idea of the simplified model is that the deformation of the bridge in direction y is approximated by a generalized degree of freedom corresponding to the first eigenmode of the bridge under sticking wheel conditions for the braked wheels of the end trucks and the trolley. This approximation implies that the higher eigenmodes of the girders are assumed to have a quasi-static response. Of course, this approximation is less satisfactory under non-linear behavior since the impact and friction forces excite higher modes also. However, this simplified model does not aim at giving high accuracy results but rather a rough but fast estimate of the crane bridge response. Consistent application of the Lagrange-Euler equations, using the above kinematic assumption, leads to a system which cannot be represented by a discrete mass system like that on figure 14. Nevertheless, numerical simulations show that the results of this mathematically more consistent model and the above "empirical" model are quite close. That is why only the results of the empirical model are presented here.

The results obtained with the simple model, subjected to the bi-axial excitation at 0.8g PGA, are shown in figure 15 and are compared with those of the FE model. For the sake of better readability the time histories in the time interval $[5\text{ s}, 7\text{ s}]$, where the peak response occurs, is presented. By construction, the simple model does not account for the different friction conditions between the braked and the free to roll wheels. Hence it cannot reproduce the asymmetric sliding response discussed in subsection 4.2. Except the sliding behavior, the

simple model, captures qualitatively the essential features of the bridge response (e.g. same response characteristic time as the FE model) but results in a mild overestimate of the response quantities. In fact, the impact forces of the two models exhibit similar, though not identical, qualitatively and quantitatively features. Regarding the relative displacement of the girder mid-point with respect to the end trucks, the simple model gives a displacement which overestimates the mean displacement of the two girder beams of the FE model by about 34%.As already mentioned in subsection 4.2, the above relative displacement is a measure of the deformation of the girders and could be used as a relevant seismic demand index for the evaluation of their seismic performance.

This simplified model could be, easily, improved further including rocking and uplift but at the price of adding supplemental degrees of freedom and higher complexity.

6. Conclusions

In this work the experimental and analytical response of a crane bridge model subjected to earthquake excitations is investigated.

Earthquake tests on a shake table of a 1/5 scale simple model of a crane bridge were carried out for different configurations (trolley location, braked or rolling wheels) under several excitations signals (bi-axial, tri-axial, growing PGA values). A novelty of the experimental campaign was the similarity law which was especially adjusted to ensure the correct ratio of seismic forces to friction forces.

A FE beam model was made. A special care must be given for the analytical model to obtain the experimentally determined eigenmodes. In particular, additional flexibilities of the girder end truck connections and of the runway beams should be taken into account.

Regarding the response under high intensity excitation, comparison between analytical and experimental results shows that, despite some discrepancies the FE model reproduces the

essential features of the nonlinear response. The overall agreement is satisfactory, especially if one recalls the well-known unpredictability of the response of nonlinear systems in the presence of severe impact/friction nonlinearities. In particular, the FE model gives a good estimate of the overall deformation of the girders (relative displacement with respect to the end trucks) which could be used as a relevant quantity, amongst others, to check the earthquake resistance of the crane bridge. Moreover, the FE model is capable to reproduce the systematic asymmetric sliding behavior of both the girders and the trolley, observed during the tests.

A simplified analytical crane bridge model is proposed which gives approximate, yet satisfactory estimates of the response quantities of interest. This model could be used as a part of a bigger model including both the support (i.e. main) structure and the crane bridge to account for possible interaction between these two structures. The simplified model cannot account for the aforementioned asymmetric sliding behavior. An extension of the simplified model, to account for this effect, could be possible but at the price of a higher complexity.

Future work will address the accurate determination of the reaction forces on the runway beams and the improvement of the analytical model. Hence, a further extension of this work would consist of some supplemental tests on shake table: a) using excitations which are closer to actual crane bridge support motions and b) equipped with suitably designed load cells to measure the reaction forces on the runway beams. Regarding the analytical model, a specific macro-element could be developed to better simulate the actual friction forces on the rolling wheels.

8. Acknowledgement

This work was partially funded by the French Institute of Radiological Protection and Nuclear Safety (IRSN).

REFERENCES

[1] Fryba L. Vibrations of Solids and Structures Under Moving Loads. Groningen: Noordhoff, 1972.

[2] Stanisic MM. On a new theory of the dynamic behaviour of the structures carrying moving masses. Ingenieur-Archiv (Archive of Applied Mechanics) 1985;55(3):176-185.

[3] Sadicu S, Leipolz HH. On the dynamics of elastic systems with moving masses. Ingenieur-Archiv (Archive of Applied Mechanics) 1987;57(3):223-242.

[4] Pesterev AV, Bergman LA. Response of elastic continuum carrying moving linear oscillator. Journal of Engineering Mechanics ASME 1997;123:878-884.

[5] Pesterev AV, Bergman LA. Vibration of elastic continuum carrying accelerating oscillator. Journal of Engineering Mechanics ASME 1997;123:886-889.

[6] Oguamanam DCD, Hansen JS, Heppler GR. Dynamics of a three-dimensional overhead crane system. Journal of Sound and Vibration 2001;242(3):411-426.

[7] Olsson M. Finite element, modal co-ordinate analysis of structures subjected to moving loads. Journal of Sound and Vibration 1985;99:1-12.

[8] Hino J, Yoshimura T, Konishi K, Ananthanarayana NA. Finite element method prediction of the vibration of a bridge subjected to a moving vehicle load. Journal of Sound and Vibration 1984;96:45-53.

[9] Komori A, Fukuda T. et al. Study on earthquake responses of overhead travelling cranes, *SMIRT* 11, 1991.

[10] Otani A, Keisuke N, Suzuki J. Vertical seismic response of overhead crane. Nuclear Engineering and Design 2002;212:211-220.

[11] Schukin A, Vayndrakh M. Seismic Non-linear analysis of Polar Crane. SMIRT 19, Toronto, August 2007.

[12] Betbeder-Matibet J, Pons JC, Labbe P, Noe H. Seismic response of sliding structures and equipment. Recent Advances in Earthquake Engineering and Structural Dynamics, Ouest Editions, Presses Académiques, 1992.

[13] Betbeder-Matibet J, Labbé P. Simplified seismic analysis methods in France. Nuclear Engineering and Design 1990;123(2–3):305-312.

[14] Sarh K, Papin MH, Guihot P. Taking into account the possibility of sliding in earthquake response of overhead cranes. 10th European Conference on Earthquake Engineering. Dums(ed.). Balkema, Rotterdam, 1995.

[15] Kenichu S., Masakatsu I and Tadashi I. Seismic Capacity Test of Overhead Crane Under Horizontal and Vertical Excitation. Journal of Disaster Research 2010; 5(4): 369-377.

[16] Harris H, Sabnis G. Structural modeling and experimental techniques. CRC Press LLC, 1999.

[17] Palmer A. Dimensional analysis and intelligent experimentation. World Scientific Publishing, 2008.

[18] Makris, N. and Black C.J, Dimensional Analysis of Bilinear Oscillators under Pulse - Type Excitations, Journal of Engineering Mechanic ASCE 2004 ; 130(9):1019-1031

[19] Makris, N., G. Kampas G. and Angelopoulou D, The Eigenvalues of Isolated Bridges with Transverse Restrains at the End-Abutments, Earthquake Engineering and Structural Dynamics 2010; 39: 869-886

[20] Chaudat T, Garnier C, Vasic S, Le Corre M, Mahe M. Seismic behavior of crane bridges-Report of experimental tests. C.E.A. Rep. No. 11-018/A, C.E.A.-Saclay, France, 2011 (in French).

[21] CAST3M http://www-cast3m.cea.fr/

[22] Peric D, Owen DR. Computational methods for for 3D contact problems with friction based on the penalty method. International Journal of Numerical Methods in Engineering 1992;35:1289-1309.

[23] Oden JT, Martins JAC. Models and computational methods for dynamic friction phenomena, Computer Methods in Applied Mechanics and Engineering 1985;52:527-634.

Table 1 Response quantities of FE models for the biaxial test at 0.8g PGA level (zero mean excitation)

Model	Reference FE model		No-tuned FE model	
Gaps	2 mm	0 mm	2 mm	0 mm
Response quantities at the girder's mid span				
Max. relative displacement (y)	1.3 mm	1.7 mm	1.1 mm	1.4 mm
Mean impact forces (y)	196 N	847 N	188 N	868 N
Max. moment (z)	4537 Nm	5314 Nm	3647 Nm	4568 Nm
Mean moment (z)	132 Nm	520 Nm	116 Nm	468 Nm
Max. axial stresses (x)	21.4 MPa	23.5 MPa	19.7 MPa	23.3 MPa
Global response quantity				
Max. sliding disp.lacement (y)	35 mm	55 mm	30 mm	45 mm

Table 1 Parameters of the simplified model

Gaps	2 mm
$m_{gi} + m_{tr}$	3648 kg × 77%
m_{tr}	1880 kg
m_e	3648 kg × 23%
Corresponding frequency for k_{gi}	9.3 Hz
Corresponding frequency for k_x	9.5 Hz
Critical damping ratio for c_{gi}	0.54 %
Restitution coefficients for c_x	0.7
Mean horizontal friction coefficient of horizontal interface	0.125
Horizontal friction coefficient of vertical interface	0.23

Figure

Click here to download Figure: Figure1.docx

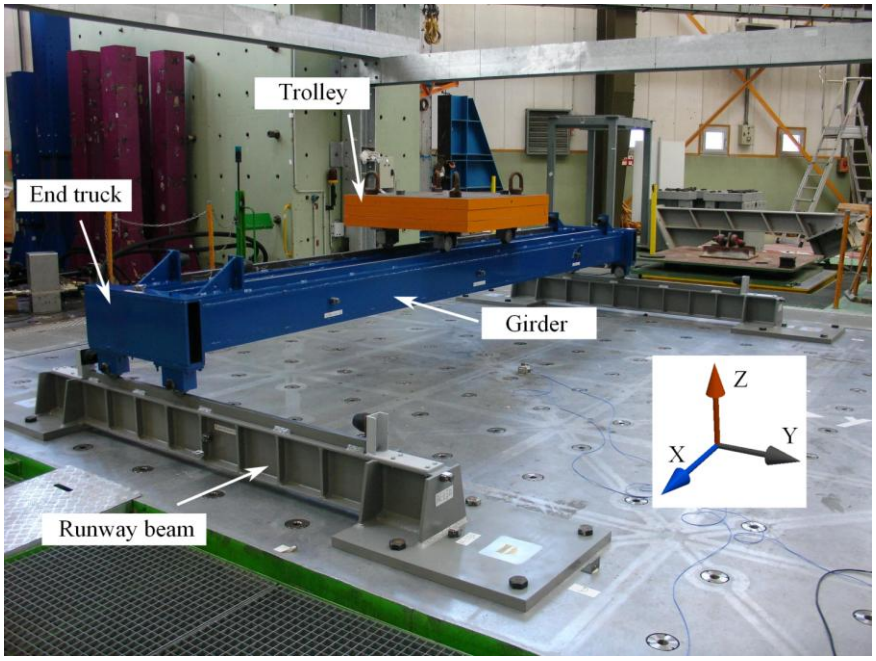

Figure 1. Model of the crane bridge mounted on the shake table.

Figure
Click here to download Figure: Figure2.docx

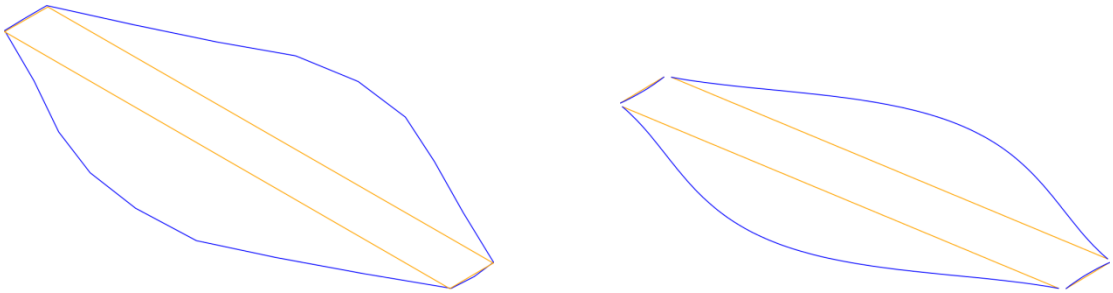

a)

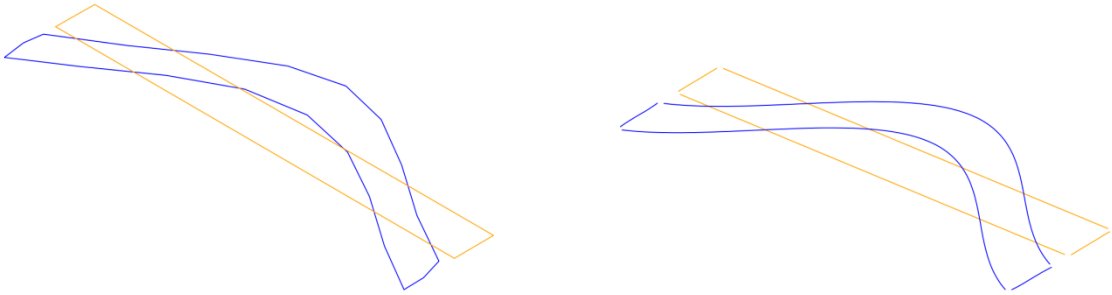

b)

Figure 2. First two eigenmodes of the subassembly composed of the main bridge girders based on the shock hammer test. Experimental results at left and analytical results at right. (a) $f_{exp.} = 18.5$ Hz vs $f_{model} = 18.2$ Hz; (b) $f_{exp.} = 32.2$ Hz vs $f_{model} = 33.8$ Hz.

Figure

Click here to download Figure: Figure3.docx

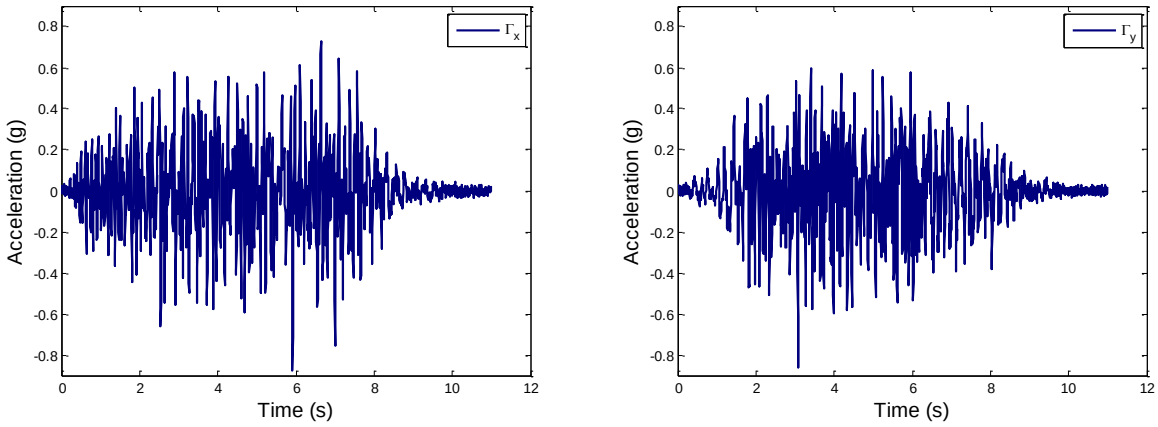

a) b)

Figure 3. Time histories of input accelerations in the case of a bi-axial test. (a) direction x; (b) direction y.

Figure
Click here to download Figure: Figure4.docx

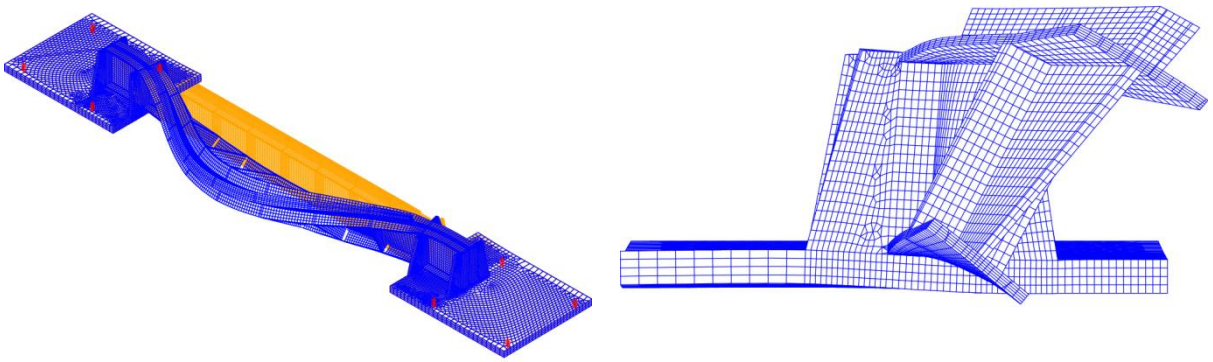

a)

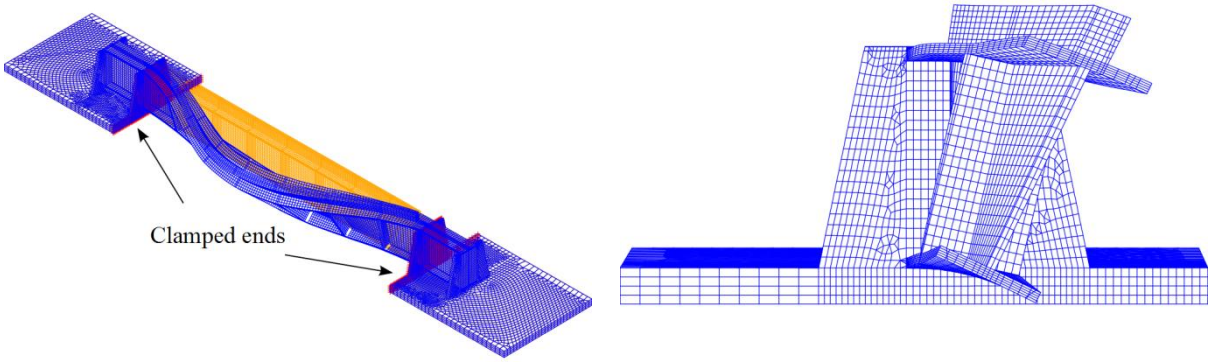

b)

Figure 4. Deformed shape of the runway beam under static loading. (a) modeling of the actual boundary conditions $f_x \simeq 9.5$ Hz; (b) beam assumed clamped at both ends, $f_x \simeq 11.5$ Hz.

Figure
Click here to download Figure: Figure5.docx

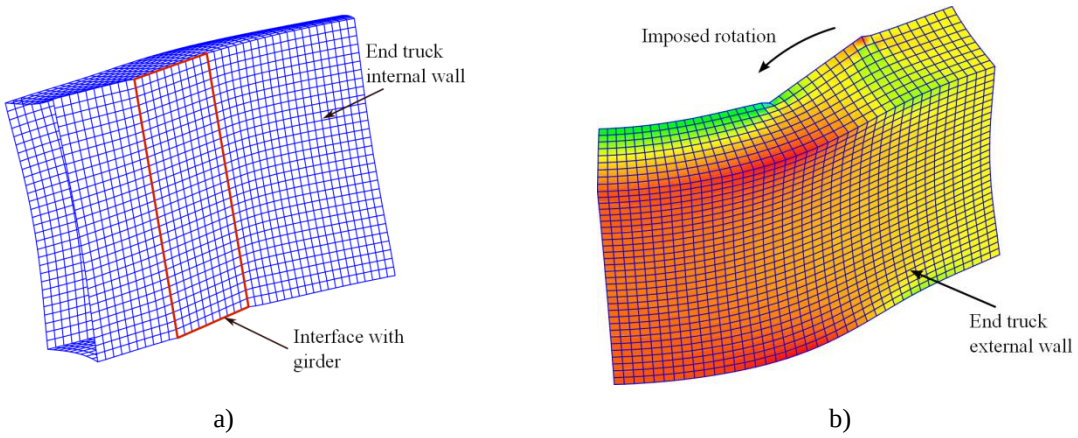

a) b)

Figure 5. Shell finite element model of the end truck. (a) mesh; (b) axial stresses distribution.

Figure
Click here to download Figure: Figure6.docx

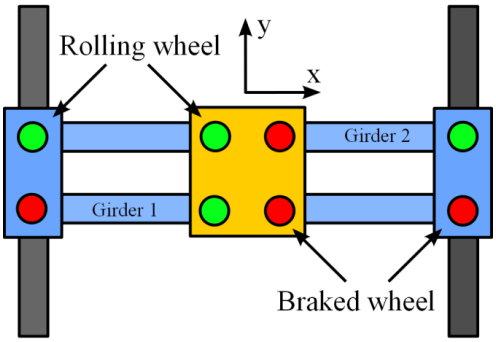

Figure 6. Configuration of braked and rolling wheels.

Figure
Click here to download Figure: Figure7.docx

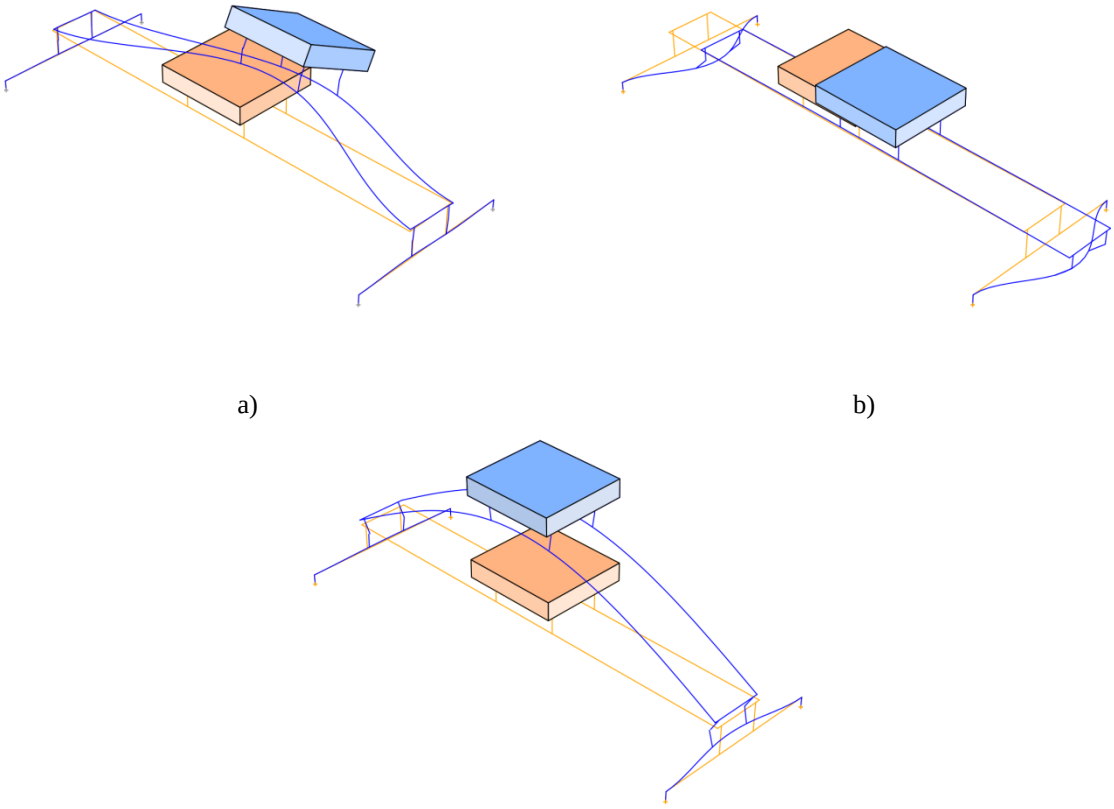

Figure 7. Mode shapes and frequencies of the finite element model of the crane bridge (frequency of the analytical model vs frequency of the specimen). (a) first mode in the y direction (9.3 Hz vs 9.5 Hz); (b) second mode in the x direction (9.5 Hz for both); (c) third mode in the z direction (14 Hz vs 13 Hz).

Figure
Click here to download Figure: Figure8.docx

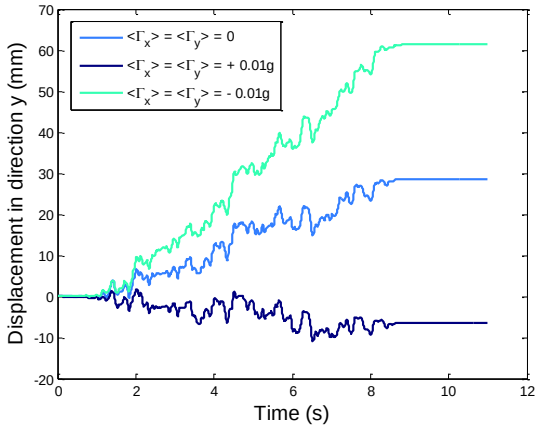

Figure 8. Mean horizontal displacements of the end trucks for different time average values, $< \Gamma_x >$ and $< \Gamma_y >$, of the excitation signals.

Figure
Click here to download Figure: Figure9.docx

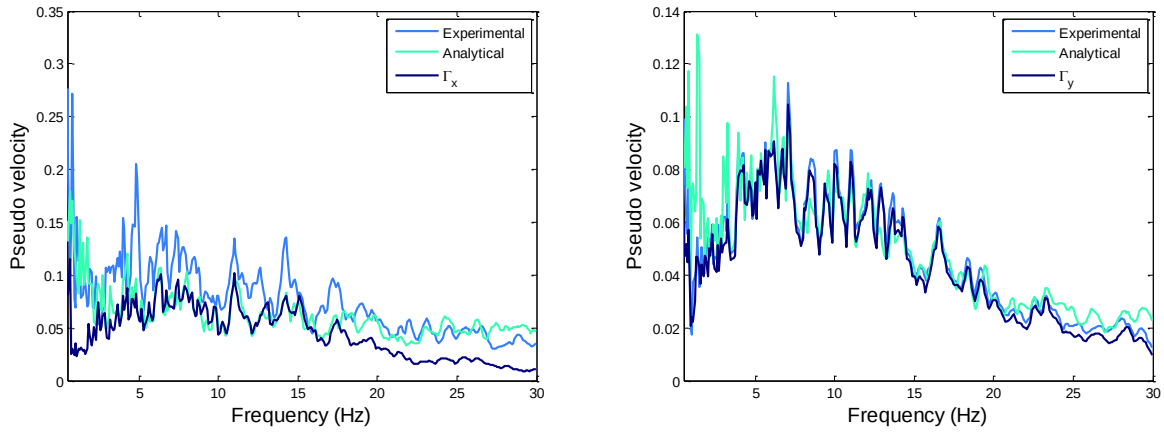

a) b)

Figure 9. Pseudovelocity response spectra of the runway beam at mid span. (a) direction x; (b) direction y.

Figure
Click here to download Figure: Figure10.docx

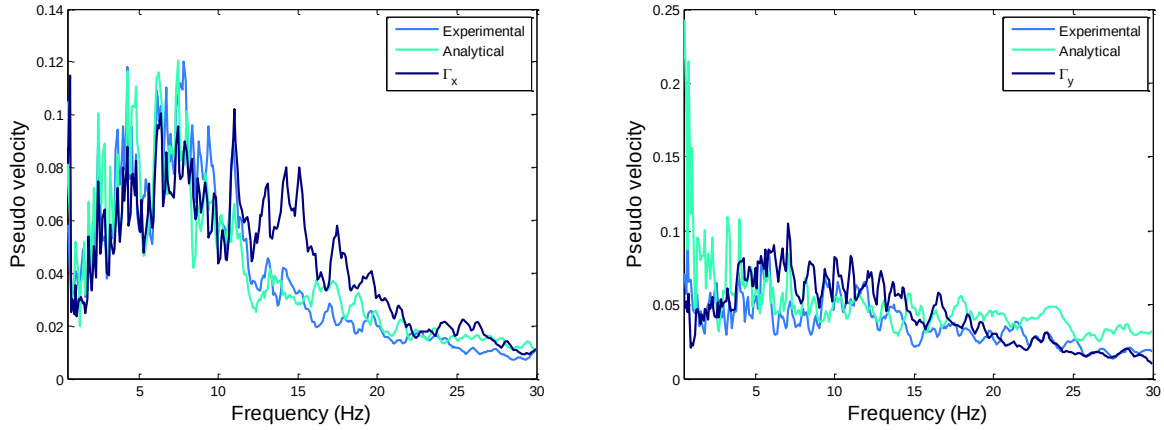

a) b)

Figure 10. Pseudovelocity response spectra of the main bridge girder at mid span. (a) direction x; (b) direction y.

Figure
Click here to download Figure: Figure11.docx

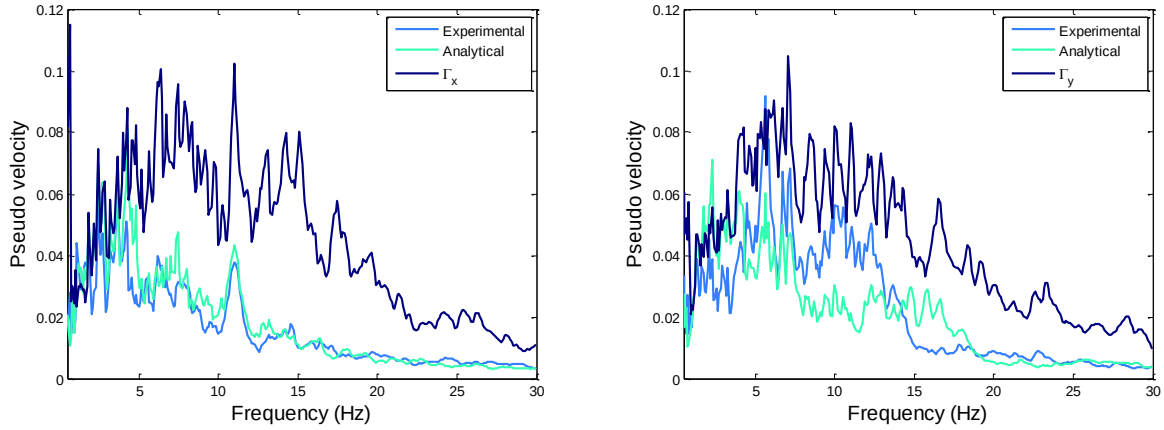

a) b)

Figure 11. Pseudovelocity response spectra of the trolley. (a) direction x; (b) direction y.

Figure
Click here to download Figure: Figure12.docx

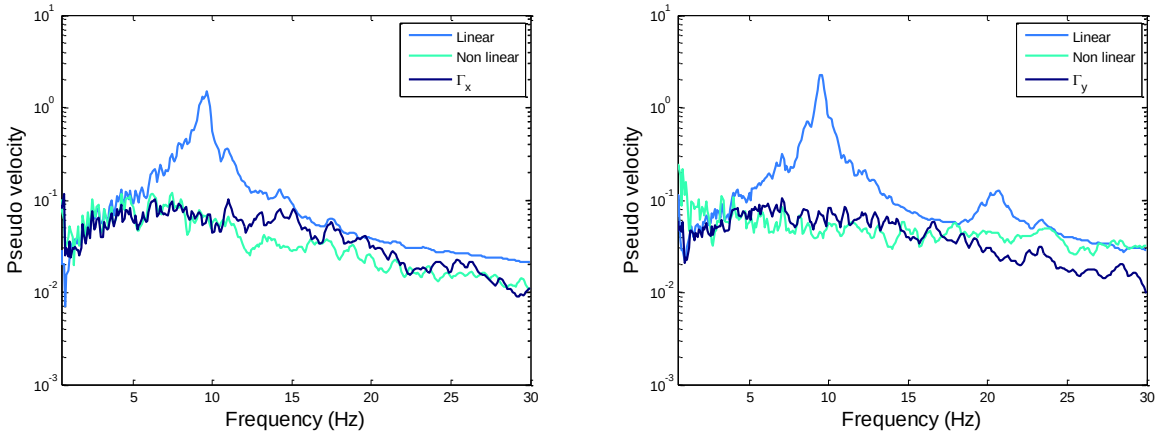

a) b)

Figure 12. Pseudovelocity response spectra of the main bridge girder at mid span. Comparison between linear and non linear results. (a) direction x; (b) direction y.

Figure
Click here to download Figure: Figure13.docx

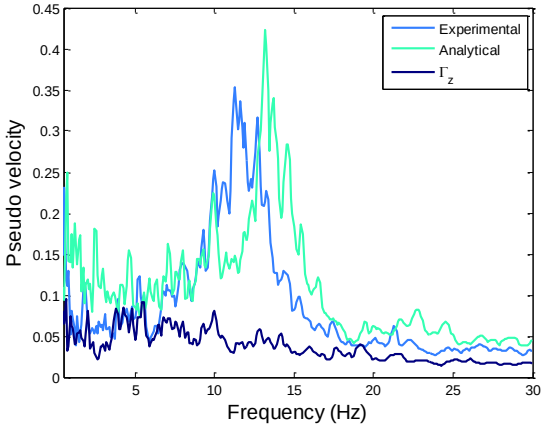

Figure 13. Pseudovelocity response spectra of the trolley in direction z. Experimental and analytical results under 3D excitation.

Figure
Click here to download Figure: Figure14.docx

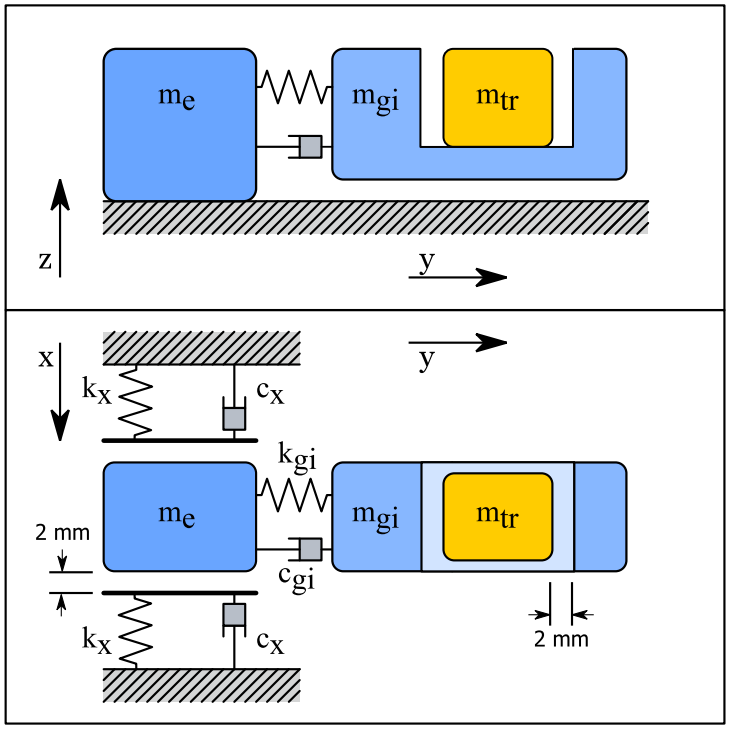

Figure 14. Simplified model.

Figure

Click here to download Figure: Figure15.docx

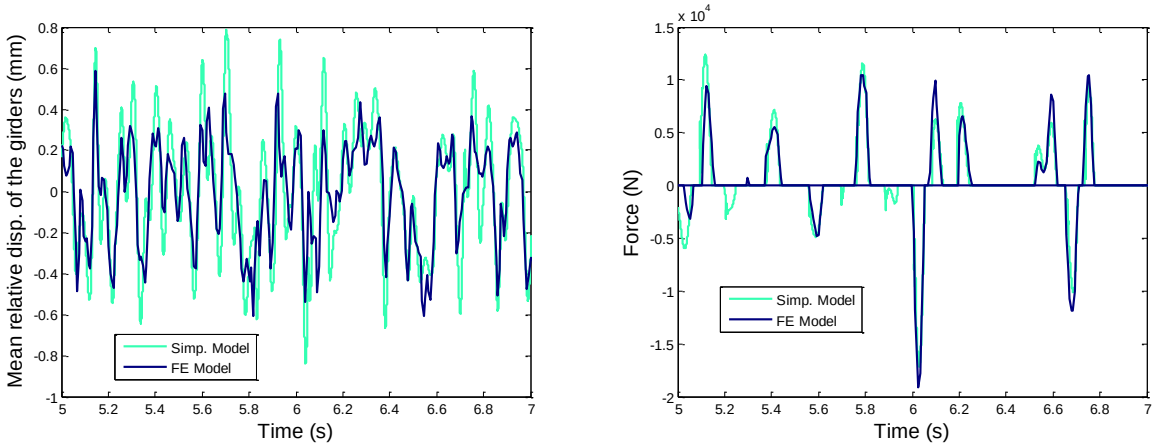

a) b)

Figure 15. Comparison between the results of simplified and FE models. (a) mean relative displacement of the girders; (b) impact forces on the runway beams.